

Vulnerability assessment of the Saudi Arabian Red Sea coast to climate change

Mohamed E. Hereher^{1,2}

Received: 11 October 2014 / Accepted: 15 July 2015 / Published online: 19 December 2015
© Springer-Verlag Berlin Heidelberg 2015

Abstract Climate changes in terms of sea level rise and global warming impose different ramifications upon the Red Sea coast of Saudi Arabia, which extends to 1840 km and witnesses accelerated urban development. The shoreline is mostly resistant to erosion and inundation by seawater due to the inherent hard nature and the relatively higher relief. Digital elevation models reveal that only about 890 km² of the coast occurs below 1 m. Global warming has a more conceivable impact upon the coast as numerous coral reef ecosystems exist, and the harm is inevitable. The coastal vulnerability index indicates that about 16 % of the coast is under high vulnerability, whereas 44 % of the coast is intimately low vulnerable to climate change. Higher vulnerable coastal segments include: relatively flat and lowlands; inhabited; and/or coral-mangrove-rich shorelines. Coastal zone management and rescue plans are essential to protect coastal resources for a long-term sustainable development.

Keywords Saudi Arabia · Coastal vulnerability index · Remote sensing · Climate change

Introduction

Coasts are among the most susceptible locations to be impacted by the global climate change, which is manifested by the global warming and sea level rise (Williams

2013). Recent investigations reported an increase in the global temperature by 0.7 °C and the rise of the sea level by 10–20 cm in the last century (IPCC 2007). Global warming is expected to continue due to the emissions of carbon dioxide (CO₂) gas into the atmosphere (Simas et al. 2001). It is expected that the sea level will rise about 60 cm by 2100 due to the thermal expansion of seawater and the melting of ice in the arctic glaciers (IPCC 2007). The dependence on the coastal zone is important worldwide as more than 60 % of the world population lives along shorelines (Doukakis 2005) and a wide range of socioeconomic activities occurs at or near coastlines. Coastal zones also contain important ecosystems and environments that maintain the ecological, nutrients, and energy balance across the globe (UNEP 1992). Although the consequences of the global climate change are not uniform and vary from one coast to another, most of the impacts include flooding, loss of lives and property, deterioration of water resources, coastal erosion, and damage of coastal ecosystems (Williams 2013). The most vulnerable coastal areas were demonstrated by flooding of lowlands (Nicholls 2002 and Hereher 2010) and impacting delicate ecosystems, such as coral reefs and mangroves (Hereher 2015a, b). Coral reefs are the most diverse among marine ecosystems (Roberts et al. 2002). They are sensitive to any change in the water temperature. Although corals favor living in warm waters, any excess of the water temperature caused by the global warming could negatively affect the algal/coral symbiosis relationship and even lead to coral bleaching and mortality (McWilliams et al. 2005). Increasing CO₂ concentrations in the atmosphere are expected to lower the ocean water pH, which could decrease coral calcic skeleton formation (Kleypas et al. 1999). Mangroves, which are the shelter for numerous birds and fish species and provide support to the

✉ Mohamed E. Hereher
mhereher@gmail.com

¹ Biology Department, Faculty of Science, The University of Hail, Hail, Saudi Arabia

² Department of Environmental Sciences, Faculty of Science, Damietta University, New Damietta, Egypt

coastline, are contingent to the tidal zone and are quite sensitive to the change in the water level and flooding (IPCC 2001). Coastal zone management is consequently an important task for sustainable development of marine resources and coasts of high ecological value (Dwarakish et al. 2009).

Coastal vulnerability assessment is an effective approach to judge the response of a given coastal segment to the consequences of climate change. The coastal vulnerability index (CVI), which was developed by Gornitz et al. (1994) is the most common and applicable method to quantify the degree of the coastal vulnerability to sea level rise (Thieler and Hammar-Klose 1999). The index is composed of individual parameters ranked along a numerical scale and multiplied together to compile a net value that represents the severity of the sea level rise upon the coast. Although the initial variables could be ranked into four classes, some other studies classified three vulnerability categories (low, medium and high) for coastal vulnerability (Kumar and Kunte 2012). Parameters utilized to calculate the CVI usually include either geologic variables, such as the geomorphology of the coast, slope, and erosion/accretion pattern or physical variables, such as the wave height, tidal range, and sea level rise records (Thieler and Hammar-Klose 2000; Pendleton et al. 2005; Boruff et al. 2005; Rao et al. 2008; Hereher 2015c). Assigning the suitable parameters within the CVI is the crucial step in the vulnerability assessment as each coastal region is characterized by its intrinsic physiographic and oceanographic attitudes. For example, in coastal areas suffering from shoreline erosion, it is important to involve historical coastline position variation within the CVI. A big limitation of the original CVI developed by Gornitz et al. (1994) is that this index rates the severity for the exposure of the coastal zone to sea level rise, but without considering the capacity of the affected communities to adapt to the projected changes (Kunte et al. 2014). Another significant limitation of the original CVI is the lacking of the variables pertaining to the biotic and the socioeconomic characteristics of the coast. Some regional studies have involved specific parameters related to the inherent behavior of the coast, e.g., tsunami amplitude (Doukakis 2005); coastal hydrology (Kumar et al. 2010); land subsidence (Ozyurt and Ergin 2010); population density (Duriyapong and Nakhapakorn 2011); storm surges (Kumar and Kunte 2012); and tourist density data (Kunte et al. 2014). Diez et al. (2007) used the coastal elevation instead of coastal slope in the coastal vulnerability assessment of the Buenos Aires Province, Argentina. Hereher (2015b) in his CVI assessment of South Sinai coast to climate change reduced the number of variables to only four parameters representing the geologic and the inherent nature of the coast. This modification was done

because South Sinai coast is under low waves and little tidal range as well as the incidence of significant coral reefs and mangroves ecosystems. The CVI suggested in this study is:

$$CVI = [(T * G * B * S)/4]^{1/2} \quad (1)$$

where T is the topography in terms of the coastal slope; G represents the geology in terms of the coastal geomorphology; B is the biota and it is related to the fauna/flora of the coast; and S is the socioeconomic factor, which concerns with the coastal land use. The calm nature of the Red Sea and its relatively raised and rocky shorelines have spurred for tailoring the parameters utilized in the CVI to match the influencing factors dominating across the coast. Each parameter has three levels of vulnerability and a corresponding numerical value: low (1.0), moderate (2.0), and high (3.0).

The Red Sea is a semi-closed basin connecting the Indian Ocean in the south with the Mediterranean Sea in the north and separating the African continent in the west from Asia in the east (Fig. 1). Maximum width of the Red Sea is about 355 km, and its minimum width is about 35 km at the Strait of Bab El-Mandab in the south. The mean depth of water is 500 m, and the tidal range is relatively low (0.2 at Jeddah to 0.8 m at Jazan) with a mean temperature of 24 °C and a salinity of 37–40 ppt (Bird 2010). Generally, oceanographic and sea level data on the Red Sea are very little. However, previous studies report that the maximum wave height is 1.8 m occurring in the southern part (Saad 2010). The Red Sea bifurcates at a latitude of 27°45'N to the Gulf of Suez in the west and the Gulf of Aqaba in the east. Saudi Arabia faces the majority of the eastern coastal plain along the Gulf of Aqaba. The warm environment, high salinity, and clarity of the water allowed for mass growth of coral reefs, where there is more than 330 coral species in this sea (Dubinsky and Stambler 2011). In addition, more than 500 species of fauna and flora have been recorded among mangroves and sea grasses in the Red Sea coast (Ellison 1999). The Red Sea is considered as one of the world's top marine biodiversity hotspots due to the natural climatic changes and anthropogenic activities (Roberts et al. 2002).

In Saudi Arabia, which has the longest coastline (about 1840 km) along the Red Sea, the coastline varies in geomorphology from cliffy shores across the Gulf of Aqaba, raised coral terraces and fringing reef coasts for the majority of the coast, to unconsolidated sediments and beaches at the south. The coastal plain in Saudi Arabia has also abundant occurrence of mangroves and sea-grasses (Price et al. 1998). The absence of perennial fluvial systems across the Red Sea has deprived the coastal plain from sediments and consequently impacted the coastal process in which coastal erosion was not

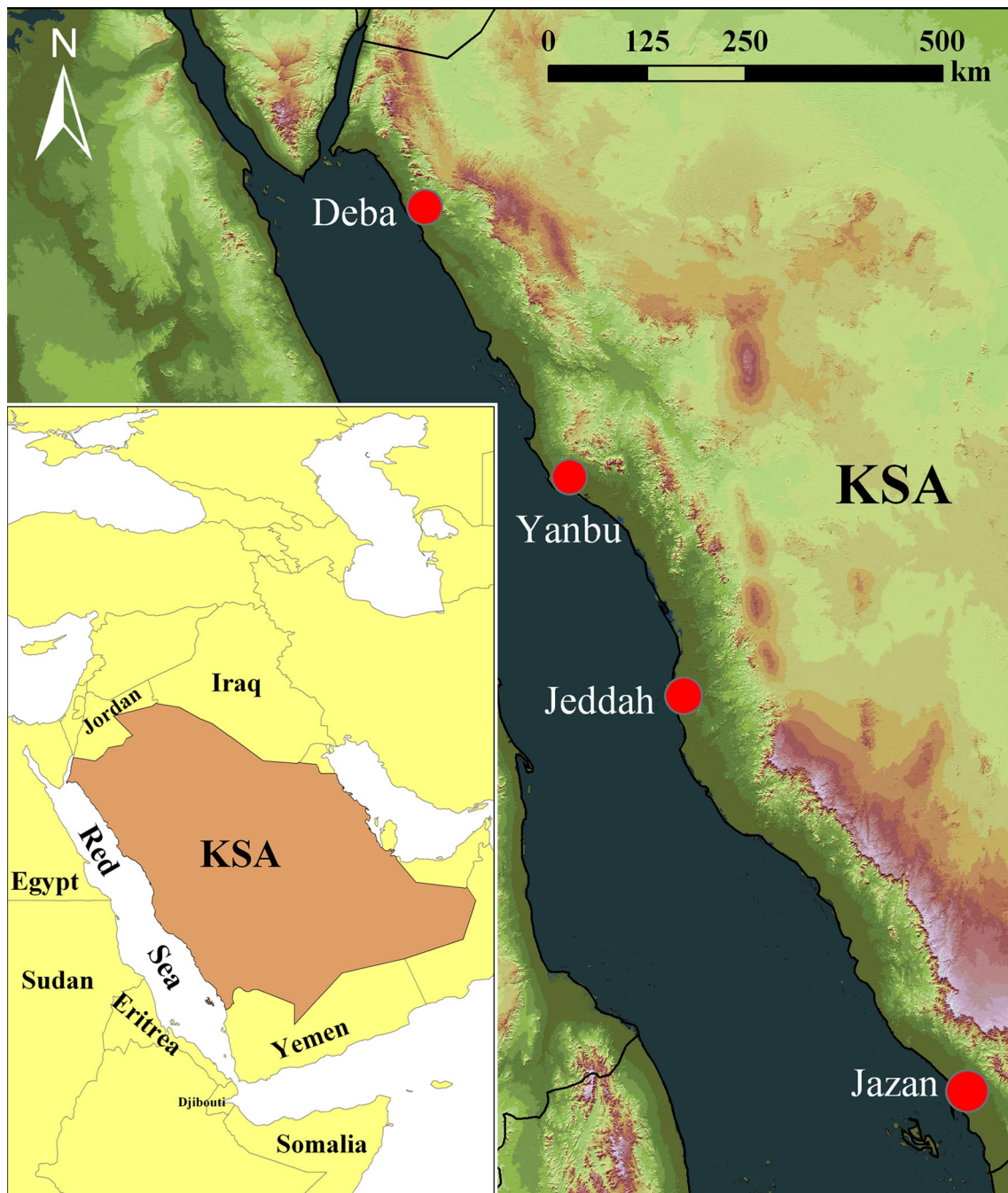


Fig. 1 Location map of Saudi Arabia showing the Red Sea coast

reported, particularly along the northern part of the Red Sea. Although the shoreline is generally rocky for the majority of its length, there is a fast-growing development of the coast with new urban communities and industrial facilities. Most of the existing cities and urban centers occur at relatively flat and near sea surface level. Saudi Arabia is one of the largest states in the world to desalinate seawater (Aburizaiza et al. 2013). Although

desalination plants are the primary source of freshwater along the Red Sea coast, disposal of cooling water represents the major threat to the marine environment with particular impact upon coral reef ecosystems. The objective of the present study is to investigate the impact of climate changes in terms of sea level rise and global warming upon the Red Sea coast of Saudi Arabia using the coastal vulnerability index.

Materials and methods

Coastal geomorphology

The makeup of the coastal materials is the key factor that likely determines the resistance and consequently the response of the coast to the wave action and storm events. Rocky and cliffy shores exhibit maximum resistance and are generally not prone to erosion, whereas unconsolidated beach sediments reveal minimum resistance to the wave action and could be easily eroded and removed from the shore. Coastal geomorphology could then provide a synoptic view and a basic understanding to the coastal environment (Kumar et al. 2010). The geomorphology of the Red Sea coast, which is contiguous to the Arabian Shield basement, was extracted from satellite images by means of remote sensing. The moderate-resolution Imaging Spectroradiometer (MODIS) images were utilized as they have a reasonable geographic coverage and spatial and spectral resolutions. Four images (h21v6, h22v6, h21v7, and h22v7) were acquired from the MODIS *Aqua* product (MYD13Q1) and dated August 13, 2014 in 250-m spatial resolution. Each image contains four spectral bands (blue, red, near-infrared, and middle-infrared) in addition to other quality and vegetation indices layers all in a HDF format within a sinusoidal projection. The spectral bands in each image were separated together in ERDAS Imagine and the four images were mosaicked to produce a single image of the entire Red Sea. In ArcGIS, the MODIS mosaic of the Red Sea was overlaid upon a DEM to identify locations of cliffs and flat beaches. The type of the shore (Table 1) was inferred by visual interpretation of the satellite images. A false color composite (FCC) using the blue, red, and near-infrared bands in the MODIS mosaic was displayed in ArcGIS, and the shore type was identified from the color tone of the shore along the entire coast. The color tone is the product of mixing the three used bands (the blue, red, and near-infrared), where each shore type has its specific spectral signature in these bands. Rocky shores have low reflection in the three bands and hence have dark tones. They were assigned a low vulnerability class (a value of 1.0). Consolidated reef shores have considerable reflection in the blue band and have a turquoise tint in the FCC. They were considered as moderate vulnerable (a value of 2.0).

Beaches and unconsolidated shorelines, which are composed of sand, have the maximum reflection in all the studied bands compared to the rocky and reef shores. They have a light tone in the FCC, and they were considered as high vulnerable (a value of 3.0). Google Earth images were used to verify the type of coastal geomorphology and to better interpret the variations of the coastal rock units.

Coastal slope

Coastal slope is the most controlling factor to delineate the inundation limit of the rising sea level or tsunami waves. Flat and gentle sloping coasts are generally susceptible to flooding by seawater, and consequently the land loss and shoreline retreat are greater in such low-sloping shores compared to those with cliffs and steep sloping ones. Coastal slope is expressed either as a percent or degrees, with most common expression in percent. The slope is the ratio of the difference in altitudinal distance to the horizontal distance of two points perpendicular to the shoreline. Coastal slope should be calculated for the entire coastal zone that is formally bordered by the line occurring at 100 km (Small and Nicholls 2003). However, in some previous studies, coastal slope was calculated for the coastal 5 km zone from the shoreline (Pendleton et al. 2005). In this study, this distance is chosen as 10 km from the shoreline as the Red Sea coast is generally narrow and most of the infrastructure such as road network occurs within 10 km from the shoreline. DEM are the most widely remotely sensed sources of acquiring information on slope and topographic aspect (Rao et al. 2008). DEM data were provided by the Shuttle Radar Topography Mission (SRTM) in 30-, 90-, and 1000-m spatial resolutions. In the present study, seven DEM tiles (43/7, 44/7, 44/8, 44/9, 45/7, 45/8, and 45/9) were obtained in 90-m spatial resolution from the Consortium for Spatial Information web portal (<http://srtm.csi.cgiar.org>). The tiles were mosaicked together in ERDAS Imagine, and a subset of the Red Sea coast was produced from which the slope in percent was determined using the *Spatial Analysis* tools in ArcGIS Software. The slope for the 10-km coastal zone was determined as pixel-to-pixel, and the maximum in this zone was recorded. Three classes of slope were assigned in relation to the vulnerability to sea level rise (Table 1) as: low (1.0) vulnerable coasts (>24 %),

Table 1 Ranges and limits of the different variables utilized to estimate the coastal vulnerability index

	Low (1)	Moderate (2)	High (3)
Coastal geomorphology	Hard rock—cliffy shores	Consolidated shores—reef shores	Unconsolidated shores—beaches
Coastal slope	<12 %	12–24 %	>24 %
Fauna/flora	Bare shores	Coastal flats	Coral reefs—mangroves
Socioeconomic	Inaccessible shores	Wide coastal plains	Cities—resorts—infrastructure

moderately (2.0) vulnerable coasts (24–12 %), and high (3.0) vulnerable coasts (<12 %).

Fauna/flora

The occurrence of the Red Sea in the subtropical zone of the world allowed for the incidence of numerous faunal and floral species along its sides. Fauna and flora in the present

study are intimately related to the coral reefs and mangrove vegetation. Locations of coral reefs were obtained from the global distribution of coral reefs database web portal (<http://www.reefbase.org>). The database was archived as Excel sheets providing the coordinates and types of the coral reefs. Locations of coral reefs were verified in finer-resolution Google Earth images and were displayed and overlaid upon MODIS images (Fig. 2). Mangrove

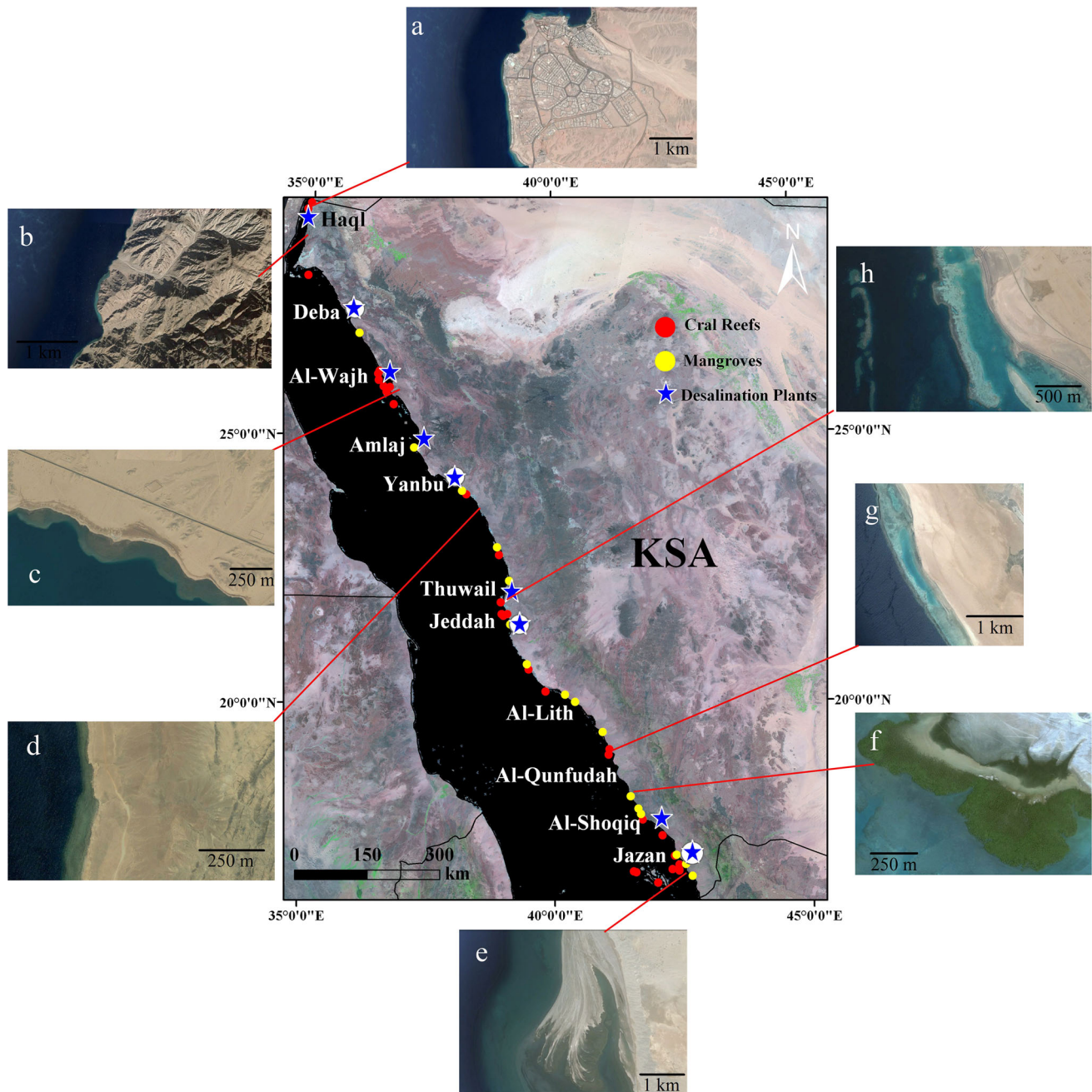


Fig. 2 Distribution of the main cities, coral reefs, and mangrove vegetation across the Red Sea. Side pictures are from Google Earth and show the following: **a** urban community at Haql along the Gulf of Aqaba; **b** cliffy shores along the gulf of Aqaba; **c** a consolidated

sedimentary shore at El-Wajh; **d** coastal flat at Sharma; **e** a coastal spit at Jazan coast; **f** mangrove at El-Qahmah; **g** fringing reef barrier at Jeddah; and **h** fringing reefs at Rabigh

vegetation was identified using spectral information of satellite data. The most accurate method to map vegetation using remote sensing is applying the normalized difference vegetation index (NDVI) using the red and near-infrared bands as vegetation has a significant absorption in the red and a sharp reflection in the near-infrared bands (Tucker 1979). The NDVI is calculated as $[(NIR - R)/(NIR + R)]$, where NIR and R refer to the reflection in the near-infrared and red bands, respectively. Green vegetation has high positive NDVI values and non-vegetation features (water, soil, urban,...etc.) have low positive, zero, or negative values. The NDVI was successfully utilized in many studies for local as well as regional mapping of vegetation (Weiss et al. 2004; Beck et al. 2006). A series of satellite images covering the entire Red Sea coast were obtained from the most recent Landsat-8 Operational Land Imager (OLI) sensor acquired in 2014. Locations of mangroves were highlighted by applying the NDVI algorithm to the OLI images and a suitable threshold for green vegetation (mangroves) in the resulted NDVI image was assigned depending on the nature of the features along the coast. The delineated threshold was 0.3, and hence, all pixels in the NDVI image equal and greater than 0.3 were recoded and grouped together as mangroves (Fig. 2). Then Google Earth images were used to verify locations of the mangrove communities along the coast. Both coral reefs and mangroves were considered as high vulnerable locations to climate change and took a value of 3.0. Bare rocky shores were considered as low vulnerable (1.0), whereas coastal flats were considered as moderate class (Table 1) as they may have coastal sabkhas and salt marshes. Thus, this category was assigned a value of 2.0.

Socioeconomic factors

Socioeconomic factors are related to the different land use across the coast, such as settlements, infrastructure, and historic locations. Coastal urban communities constructed at flat and near sea level locations are more vulnerable to flooding, particularly during tsunami waves. Any coastal vulnerability assessment should incorporate the weight that the socioeconomic impact could exert as any damage or loss of property is translated to money. In previous studies, Kunte et al. (2014) considered population and tourist density as vulnerable coastal sites. Google Earth images were utilized to identify the coastal face of urban communities and infrastructure along the Red Sea coast. Locations of urban land use were considered as high (3.0) vulnerable to sea level rise as they mostly occur near the sea level (Table 1). Inaccessible and rugged topography coasts are considered as low (1.0) vulnerable class, whereas accessible and wide coastal plains are considered as moderately (2.0) vulnerable as they have a potential for

urbanization. Locations of desalination plants were also identified in order to highlight anthropogenic impacts upon coastal waters.

Coastal vulnerability index (CVI)

After delineating the vulnerability degrees of the individual parameters, the numerical value for each level was assigned to delimit low, moderate, and high vulnerability classes as 1, 2, and 3, respectively. GIS was utilized to highlight the location and value of each vulnerability class by the *polyline* function tools in ArcMap, and then four maps showing the individual parameters were prepared. An attribute table for the vulnerability ranks of each variable with their corresponding values was constructed for each coastal segment. With the aid of the *Spatial Analysis and Overlay* functions in ArcMap, the variables were integrated together to calculate the CVI using Eq. (1) as the square root of the product of the ranked four variables (Table 1) divided by four. The resulted number determines the weight of the response of each coastal segment to climate change. Scaling of the resulted number was carried out using the percentile analysis (Thieler and Hammar-Klose 1999). The CVI classes were sliced by ranking all the resulted CVI values according to the 33rd and 66th percentiles, as low CVI (<33rd percentile); moderate CVI (33rd–66th percentiles); and high CVI (>66th percentile). In this study, the 33rd and the 66th percentiles were fixed at 1.8 and 3.0, respectively. Therefore, the vulnerability scale is low (CVI <1.8); moderate (1.8–3.0); and high (CVI >3.1). For example, if a coastal zone has the following levels of coastal parameters: high (3.0) for geomorphology (e.g., beach sand); high (3.0) for coastal slope (gentle sloping); low (1.0) for fauna/flora (bare shore); and moderate (2.0) for socioeconomic factor (wide coastal plain), then the resulted CVI is 2.12, which means that the coast at this region has a moderate sensitivity to climate change. A CVI map showing the possible synoptic reaction of the Red Sea coast to any anticipated climate change was prepared.

Results

From the geomorphological point of view (Fig. 3), the high vulnerable coastal segment accounts for the southern 210 km (11.4 % of the coast), where beaches dominate. The low vulnerable shorelines comprise the cliffy and rocky shores which occur along 458 km (25 % of the coast). The remaining 1172 km (63.4 %) of the coast has a moderate geomorphological vulnerability to the sea level rise as they are composed of corals and reef terraces. The coastal slope vulnerability (Fig. 3) is generally high for

about 1120 km (60 % of the coast) as the slope gradient is less than 12 %, whereas cliffy and steep sloping shores represent 216 km (11.7 %) and mostly occur along the Gulf of Aqaba. Coral reefs have been recorded in about 38 locations across the coast mostly of the fringing reef types (<http://www.reefbase.org>). Most coral assemblages are concentrated at El-Wajh at the north, Jeddah at the middle, and along Farasan Island at the south (Fig. 2). On the other hand, NDVI analysis reveals the occurrence of 17 sites of mangroves mostly at the southern part near Jazan. Both the coral reef and mangrove ecosystems, which are considered of high vulnerability class represent about 890 km (48 % of the coast) (Fig. 4). Low vulnerability shorelines represent 420 km (22.8 %) and those include cliffy shoreline, where marine organisms require special means of attachment to the shorelines. The socioeconomic vulnerability is highest for the coastal faces of the cities and resorts along the Red Sea, which total 393 km (21.3 %) (Fig. 4). The longest coastal face is encountered along the city of Jeddah (90 km). Moderately vulnerable coasts with economic value, which have wider coastal plains are observed for 961 km (52.2 %), whereas the least vulnerable shorelines occur along the northern part of the Red Sea at the inaccessible cliffy shorelines (27.5 % of the coast).

Calculated CVI (Fig. 5) shows that the minimum value is 0.5 and occurs along the Gulf of Aqaba, where the

coastal geomorphology includes hard rocky shores; the coastal slope is steep; the shore is void of sensitive fauna/flora ecosystems, and there is no significant land use on the coast. On the other hand, maximum CVI is 4.5 occurring at Jazan region, where there is a sandy beach with conspicuous coastal spits (Fig. 2) of very low resistance to wave action and inundation; the shoreline is rich in mangroves, the nearshore zone is flourished with coral reefs, and the area is under different land uses. Low CVI (<1.8) accounts for 733 km (40 %) of the coast and occurs mainly along the northern Red Sea coastal plain. Moderate CVI (1.8–3.0) covers the majority of the coastal plain for 801 km (44 %), whereas high CVI (>3.1) incorporates 306 km (16 %) of the coast. High CVI coasts are observed at six locations: Yanbu; Thuwail; Jeddah; Al-Qunfudah; and Jazan. All these are coastal cities with relatively flat shores and are rich in biological diversity (corals or mangroves). To validate the calculated CVI with field observations two populated coastal regions with different CVI values were inspected. These two regions are Yanbu (high CVI) and Amlaj (low CVI). Field observations revealed that the coast at Yanbu is relatively flat with extended backshore and gentle sloping, whereas the coast at Amlaj is narrow, rocky, and the backshore is flanked by a mountainous range (Fig. 6). Results showed that field observations coincide with the calculated CVI.

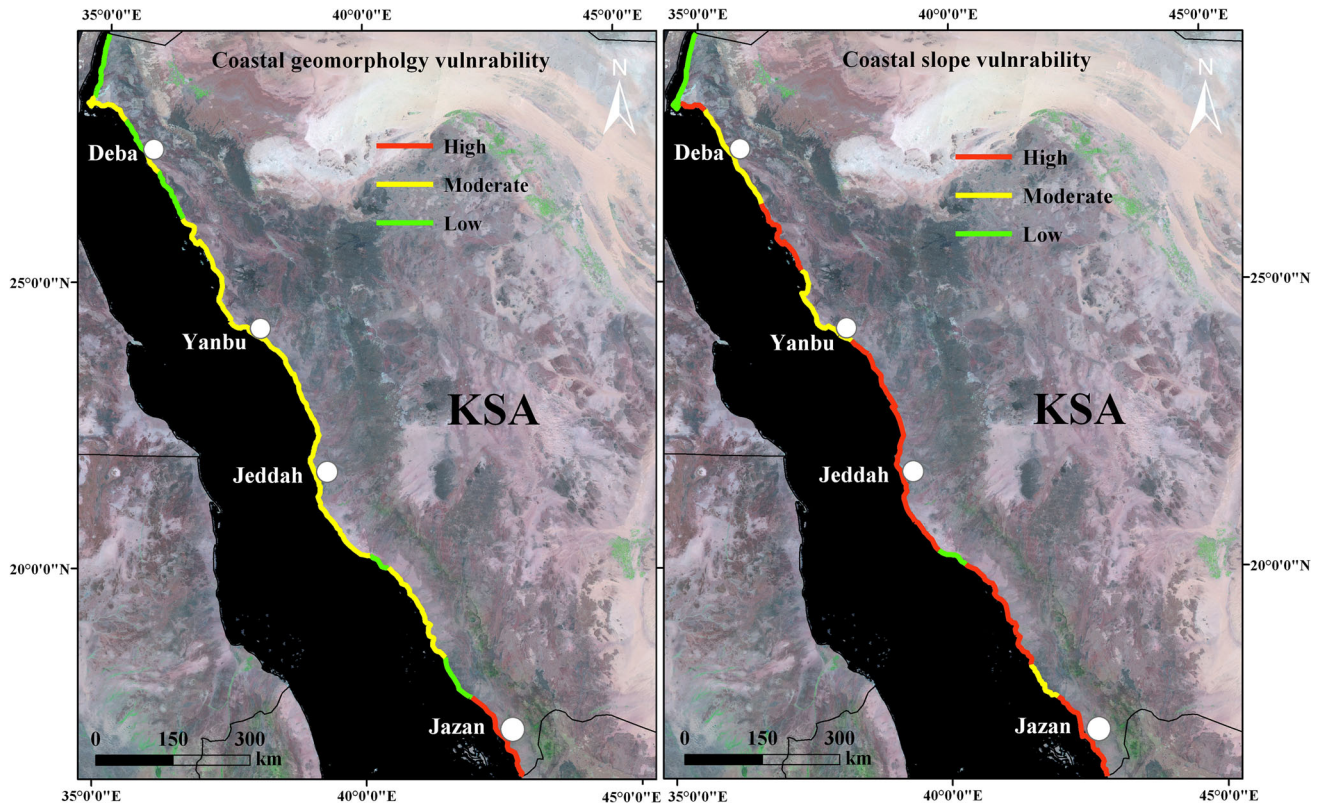


Fig. 3 Coastal geomorphology vulnerability classes (left) and the coastal slope vulnerability classes (right) along the Red Sea coast

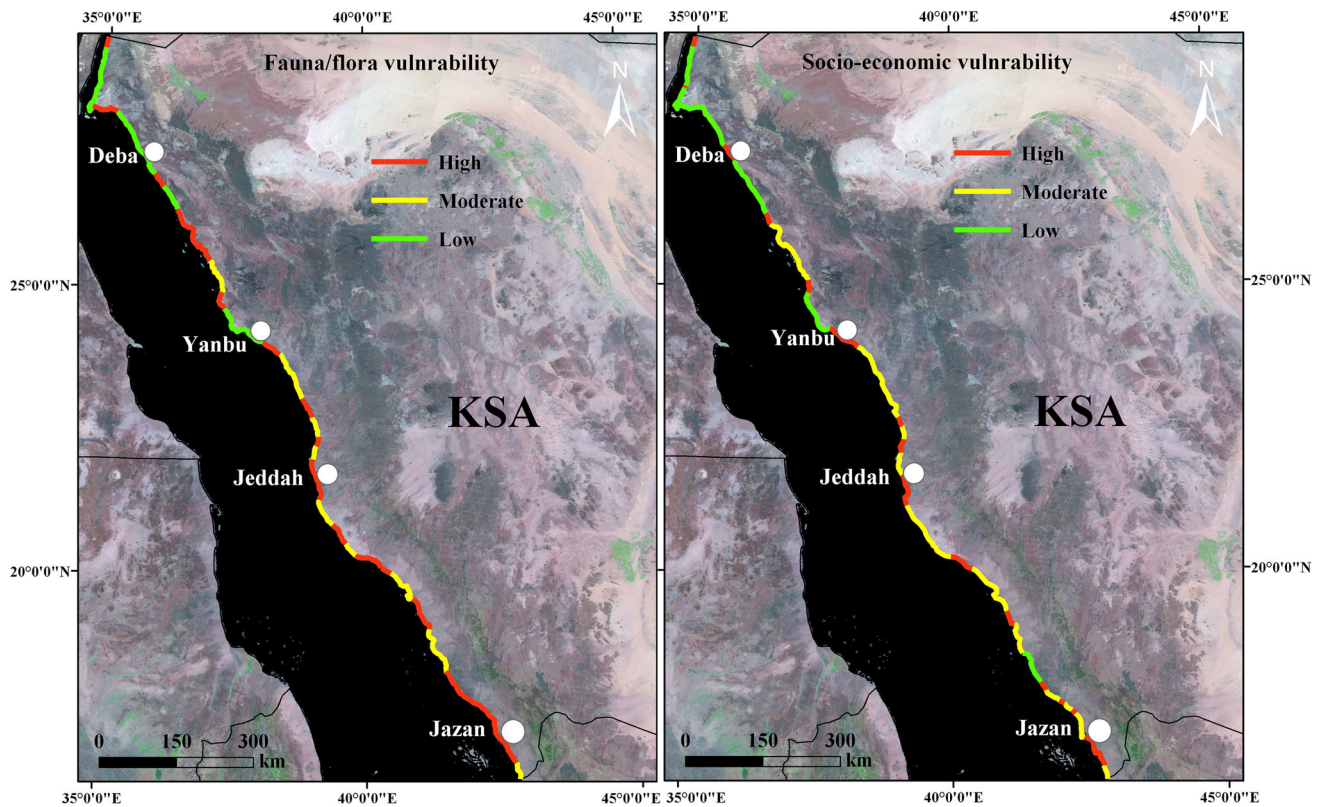


Fig. 4 Fauna/flora vulnerability classes (*left*) and the socioeconomic vulnerability classes (*right*) along the Red Sea coast

Discussions

The Red Sea coastal plain

The Red Sea occurs in a rift basin separating the African from the Arabian tectonic plates (Bosworth et al. 2005). The coastal plain of Saudi Arabia reveals a conspicuous uplifting in numerous locations that could be attributed either to the Tertiary tectonism or to the transgressions of the sea level. This uplifting is manifested by the occurrence of frequent coral limestone terraces above the current sea level, particularly along the northern part of the Red Sea coast (Behairy 1983). The coast borders a rugged mountainous range composed of igneous and metamorphic basement complex; the Arabian Shield. The Gulf of Aqaba coast is the area where these igneous and metamorphic rock units shape the shoreline. There, the coast is barely accessible except for some localities, such as Haql in the north. The rocky nature coupled with the raised coralline terraces is considered a natural defense against waves and storms, and this may explain why coastal erosion was not reported. The Red Sea coastal plain is generally narrow, about 5 km, from Yanbu to Jeddah. It widens southward of Jeddah to a maximum width of about 50 km near Jazan. The shoreline at Jazan region is composed of sediments brought to the coast by the valleys originating in Asir

Highlands, e.g., Wadi Baysh and Wadi Sabya (Vincent 2008). Environmental conditions in Jazan area coast are most favorable for mangrove flourishing than in the northern section (Saifullah 1994; Price et al. 1998). The Red Sea coast experiences accelerated urban development; however, agricultural activities are absent due to the limited freshwater supply that is barely devoted to municipal uses.

Impacts of the sea level rise

Sea level rise is one of the global climate induced problems that threaten significant coastal areas in the world. For example, the rise in the sea level by 1 m could inundate about 31 % of the entire Nile Delta (Hereher 2010). Sea level rise represents a considerable concern to flat beaches composed of sand and mud sediments. Coastal erosion and land loss; inundation of coastal wetlands and lowlands; and deterioration of freshwater resources as well as other socioeconomic ramifications are the primary consequences of rising of the sea level (Nicholls 2002). In the Saudi Arabian western coast, the consolidated and raised beaches are considered stable barriers against wave storms; however, lowlands could easily be overwhelmed by any rise of the sea level. With taking into consideration the annual recorded sea level rise (1.8 mm, Church et al. 2004) and as

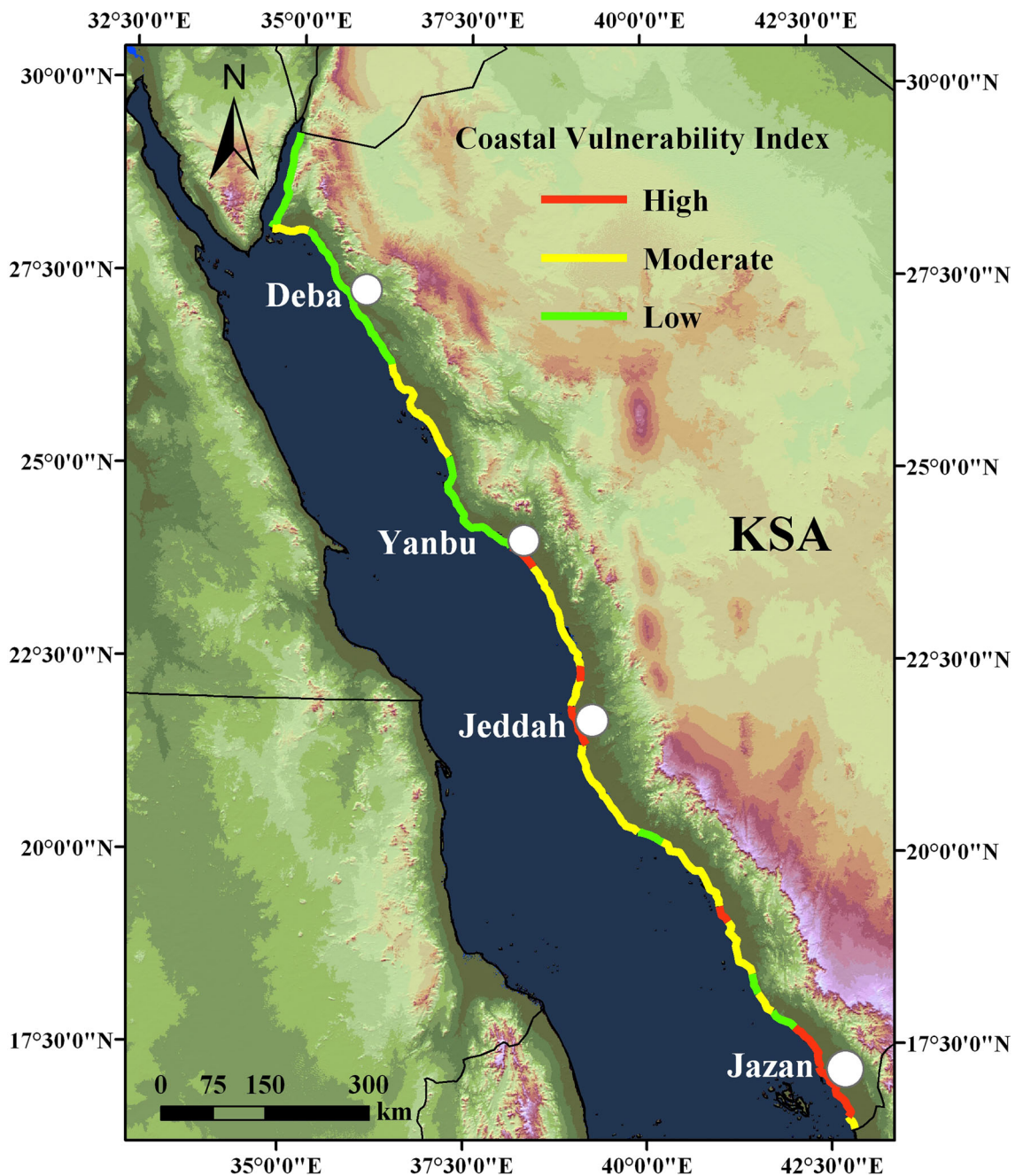


Fig. 5 Coastal vulnerability index (CVI) map of the Red Sea coast

expected that the sea level will rise by 60 cm by 2100 (IPCC 2007), projections of the sea level rise along the Red Sea coast are not significant. DEM data reveal that lowlands (<1 m level) account for an area of only 890 km² along the entire coast. If the sea level rises by 2 and 3 m, these levels should flood 2075 and 3335 km² of the coastal area, respectively. In the worst case and if tsunami waves strike the coast with up to 4 m height tides, the total area to be inundated is 4538 km², which represents a narrow coastal strip with maximum width of about 6 km from the

shoreline. The most vulnerable locations to seawater flooding is the coastal strip between Yanbu and Jeddah and Jazan coast (Fig. 7). In addition to the urban land use across these segments, mangrove forests should also be affected. Farasan Island is one of the important marine sanctuaries in the Red Sea, where coral reefs and domestic birds inhabit this island. The rise in the sea level should flood significant area of the island and could overwhelm 26 % of the famous birds Kentish plover nests (AlRashidi et al. 2012).

Fig. 6 Ground photographs of Amlaj (a) and Yanbu (b) coasts. Note that Amlaj is bordered from the west by mountains and Yanbu coast is flat



Impacts of global warming

The excess emission of CO_2 gas into the atmosphere has increased the gas concentration in the ocean water, which in turn could increase the ocean acidification (Hoegh-Guldberg 2011). Coral reefs communities, which are made up of calcareous skeletons should exacerbate from the change in the water pH. Calcification rates of reef-building materials should consequently be reduced. The greenhouse gasses, mostly H_2O and CO_2 , which are responsible for increasing the atmospheric and ocean temperature, could seriously cause reef bleaching, which usually occurs when temperatures exceed a $0.8\text{--}1\text{ }^\circ\text{C}$ above the mean summer levels for at about 4 weeks (Hoegh-Guldberg 1999). Some recent studies have shown slowing and even death of coral reefs in the Red Sea due to global warming (Sheppard 2003; Cantin et al. 2010). There are three important regions with significant clusters of coral reefs along the Red Sea coast of Saudi Arabia, Al-Wajh in the north, Jeddah in the middle, and along Farasan Island near Jazan in the south. The reef coast is not only providing a habitat for several marine species, but it acts also as a natural protection fence against wave surges and high storms. Global warming of the seawater could lead to mass coral bleaching in the Red Sea. Therefore, the Red Sea should be considered a threatened location due to global warming.

Impacts of anthropogenic activities

The Red Sea coast of Saudi Arabia is witnessing accelerated urban development, where many desalination plants, power stations and wastewater treatment facilities are being constructed each year. Desalinized water from the Red Sea is the primary source of freshwater for the western side of the Kingdom, where there is a daily production of 3.29 million m^3 of desalinized water (Aburizaiza et al. 2013). The disposal of the brine water from desalination plants would increase the seawater salinity to the degree that could intimidate and harm marine organisms. On the other hand, the disposal of untreated, partially treated or even treated wastewater into the Red Sea from coastal resorts would dilute seawater in the coastal zone that also could threaten living organism in this marine environment. Heavy metal pollution from untreated wastewater was reported in Jeddah area (Hakami and Abu Seif 2014). The discharge of cooling water from desalination plants and power stations across the coast is the major threat and may be fatal to coral reefs in the nearshore zone. Oil spill is another human-induced threat that could impact the Red Sea coastal plain, because the Red Sea is a major rout of transporting oil between the Arabian Gulf and the western world.

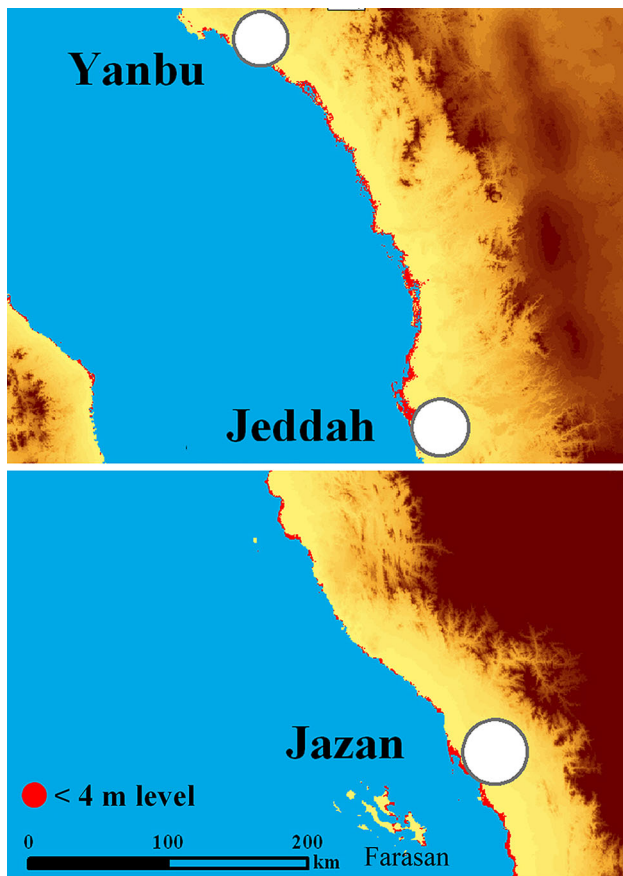


Fig. 7 Coastal areas below 4 m across the Jeddah and Jazan coastal strips

Coastal zone management

The Red Sea coastal zone constitutes a spectacular interface between mountainous terrestrial and marine ecosystems. Understanding the nature of the impact that climate changes (sea level rise/global warming) could exert is important for effective and successful coastal zone management. The elevated and reef nature of the Red Sea coast reveal that the majority of the coast is less prone to sea level rise, where geological controls support and save shorelines from the high tidal wave storms. Coastal protection measures, yet, should be implemented in areas, such as Jeddah and Jazan to confront sudden wave storms. Jeddah, which is the second largest city in Saudi Arabia, with a total population exceeding 3 millions, was built upon a plateau of up to 10 m above the sea level; however, extensions of the city occur north and south along the flat coastal plain. Such extensions should take into account the risk of flooding. Rescue centers and well-equipped coastal management facilities should be constructed near resort centers. On the other hand warming of the seawater, either by natural or anthropogenic factors, has an utmost priority for consideration and adaptation along the coast. The

coastal zone should be categorized into: I—areas under the impact of sea level rise and II—others under the threat of seawater warming. The first category includes coastal cities at relatively low elevation, such as Jeddah and Jazan, and the mangrove vegetation sites. The second category comprises the hotspot localities, which include significant coral reef assemblages in El-Wajh, Jeddah and Farasan and the locations where warm and brine wastewater are disposed into the sea. Adaptive plans are needed to safeguard threaten sites and to provide alternative solutions for cooling hot water in desalination and power plants before transmitting to the sea. Public awareness and community alert programs are important to coastal inhabitants and management officers. New desalination plants should be established in areas far from coastal coral reefs. Cooling water from desalination and power station plants should reside a longer time on land before final disposal into the sea. Institutional plans should be tailored to afford coastal regulations for fishing, tourism, industrial, and urban activities at sensitive locations. Marine and coastal protected areas are suggested in areas such as northern Jeddah coast in order to protect coral reef communities. Research centers are also required to provide scientific consultancy for siting suitable locations of urban and desalination plants. Executive plans are important to initiate an integrated coastal zone management in the region.

Conclusions

When the sources of data are little, remote sensing could afford sufficient information, particularly for regional mapping of coastal areas. The present study is performed on level-1 surveying (regional scale), in which accuracy of remotely sensed data could be reasonable and in a costly effective manner (Appelquist and Balstrøm 2014). Coastal vulnerability index is one of the effective approaches to rate coastal sensitivity to the consequences of climate change. About 16 % of the 1840-km-long Saudi Arabian coast is under high vulnerability to climate change. The geological setting of the coast plays a crucial rule that determines the reaction with any anticipated climate change. The coast is mostly narrow, elevated and adjacent to basement complexes that likely make the shoreline resistant to the ramifications of the sea level rise. However, coastal cities at lowlands and mangrove communities should respond negatively. The geographic location, climate, and absence of ephemeral streams terminating along the Red Sea allowed for the occurrence of significant clusters of coral reefs, which are sensitive to global warming. Three important locations are to be alerted: Al-Wajh, Jeddah, and Jazan. In general, the projected climate change will alter the environmental conditions along the

Red Sea coast and thereby coastal zone management plans are needed to protect vulnerable locations.

Acknowledgments This research was funded by the Deanship of Scientific Research, The University of Hail, Saudi Arabia—Project number: SCBI-17. The author also acknowledges two anonymous reviewers for suggesting valuable comments and for their deep revision of the manuscript.

References

- Aburizaiza O, Zaigham N, Gohar Z, Mahar A, Siddiq A, Noor S (2013) Environmental assessment of natural & anthropogenic hazards and impact on seawater desalination along Red Sea coast of Saudi Arabia. *J Water Resour Prot* 5:414–426
- AlRashidi M, Shobrak M, Al-Eissaa M, Székely T (2012) Integrating spatial data and shorebird nesting locations to predict the potential future impact of global warming on coastal habitats: a case study on Farasan Islands, Saudi Arabia. *Saudi J Biol Sci* 19:311–315
- Appelquist L, Balstrøm T (2014) Application of the coastal hazard wheel methodology for coastal multi-hazard assessment and management in the state of Djibouti. *Climate Risk Manag* 3:79–95
- Beck P, Atzberger C, Høgda K, Johansen B, Andrew S (2006) Improved monitoring of vegetation dynamics at very high latitudes: a new method using MODIS NDVI. *Rem Sens Environ* 100:321–334
- Behairy A (1983) Marine transgressions in the west coast of Saudi Arabia (Red Sea) between mid-Pleistocene and present. *Marine Geol* 52:25–31
- Bird E (2010) Saudi Arabia, Red Sea Coast. *Encyclopedia of the World's Coastal Landforms*. Springer Science + Business Media. doi:10.1007/978-1-4020-8639-7_16.1
- Boruff BJ, Emrich C, Cutter SL (2005) Erosion hazard vulnerability of US coastal counties. *J Coastal Res* 21:932–943
- Bosworth W, Huchon P, McClay K (2005) The Red Sea and Gulf of Aden Basins. *J Afr Earth Sci* 43:334–378
- Cantin NE, Cohen AL, Karnauskas KB, Tarrant AM, McCorkle DC (2010) Ocean warming slows coral growth in the central Red Sea. *Science* 329(5989):322–325
- Church J, White N, Coleman R, Lambeck K, Metrovica J (2004) Estimates of the regional distribution of sea level rise over the 1950–2000 period. *J Clim* 17:2609–2625
- Diez PG, Perillo GME, Piccolo MC (2007) Vulnerability to sea-level rise on the coast of the Buenos Aires Province. *J Coast Res* 23:119–142
- Doukakis E (2005) Coastal vulnerability and risk parameters. *Eur Water* 11(12):3–7
- Dubinsky Z, Stambler N (eds) (2011) *Coral reefs: an ecosystem in transition*. Springer Science, Heidelberg
- Duriyapong F, Nakhapakorn K (2011) Coastal vulnerability assessment: a case study of Samut Sakhon coastal zone. *Songklanakarin J Sci Technol* 33:469–476
- Dwarakish GS, Vinay SA, Natesan U, Asano T, Kakinuma T, Venkataramana K, Pai BJ, Babita MK (2009) Coastal vulnerability assessment of the future sea level rise in Udipi coastal zone of Karnataka state, west coast of India. *Ocean Coast Manag* 52:467–478
- Ellison J (1999) Impacts of sediment burial on mangroves. *Mar Pollut Bull* 37:420–426
- Gornitz VM, Daniels RC, White TW, Birdwell KR (1994) The development of coastal risk assessment database: vulnerability to sea-level rise in the US southeast. *J Coast Res* 12:327–338
- Hakami B, Abu Seif E (2014) Geo-Environmental Assessment of Hazardous Effects of Disposal Wastewater, Jeddah, Red Sea Coast, Saudi Arabia. *Int J Innov Res Dev* 3:170–179
- Hereher M (2010) Vulnerability of the Nile Delta to sea level rise: an assessment using remote Sensing. *Geomat Nat Hazards Risk* 1:315–321
- Hereher M (2015a) Assessment of Egypt's Red Sea coastal sensitivity to climate change. *Environ Earth Sci* 74:2831–2843. doi:10.1007/s12665-015-4304-z
- Hereher M (2015b) Assessment of South Sinai coastal vulnerability to climate change. *J Coast Res* 31(6):1469–1477. doi:10.2112/JCOASTRES-D-14-00018.1
- Hereher M (2015c) Coastal vulnerability assessment of Egypt's Mediterranean coast. *Geomat Nat Hazards Risk* 6(4):342–355
- Hoegh-Guldberg O (1999) Climate change, coral bleaching and the future of the world's coral reefs. *Mar Freshw Res* 50:839–866
- Hoegh-Guldberg O (2011) Coral reef ecosystems and anthropogenic climate change. *Region Environ Change* 11:215–227
- IPCC (2001) *Climate change 2001: the scientific basis*. Contribution of Working Group I to the Third Assessment Report of the Intergovernmental Panel on Climate Change. In: Houghton JT, Ding Y, Griggs DJ, Noguer, M, van der Linden PJ, Dai X, Maskell K, Johnson CA (eds) Cambridge University Press, Cambridge, New York
- IPCC (2007) *Climate Change 2007: Impacts, Adaptation and Vulnerability*. Contribution of Working Group II to the Fourth Assessment Report of the Intergovernmental Panel on Climate Change. In: Parry ML, Canziani OF, Palutikof JP, van der Linden PJ, Hanson CE (eds) Cambridge University Press, Cambridge
- Kleypas JA, Buddemeier RW, Archer D, Gattuso JP, Langdon C, Opdyke BN (1999) Geochemical consequences of increased atmospheric carbon dioxide on coral reefs. *Science* 284(5411):118–120
- Kumar A, Kunte P (2012) Coastal vulnerability assessment for Chennai, east coast of India using geospatial techniques. *Nat Hazards* 64:853–872
- Kumar TS, Mahendra RS, Nayak S, Radhakrishnan K, Sahu KC (2010) Coastal vulnerability assessment for Orissa State, East Coast of India. *J Coast Res* 26:523–534
- Kunte PD, Jauhari N, Mehrotra U, Kotha M, Hursthouse AS, Gagnon AS (2014) Multi-hazards coastal vulnerability assessment of Goa, India using geospatial techniques. *Ocean Coastal Manag* 95:264–281
- McWilliams JP, Cote IM, Gill JA, Sutherland WJ, Watkinson A (2005) Accelerating impacts of temperature-induced coral bleaching in the Caribbean. *Ecology* 86(8):2055–2060
- Nicholls RJ (2002) Analysis of global impacts of sea-level rise: a case study of flooding. *Phys Chem Earth* 27:1455–1466
- Ozyurt G, Ergin A (2010) Improving coastal vulnerability assessments to sea-level rise: a new indicator-based methodology for decision makers. *J Coast Res* 26:265–273
- Pendleton EA, Thieler ER, Williams SJ (2005) *Coastal Vulnerability Assessment of Golden Gate National Recreation Area to Sea-Level Rise*. U.S. Geological Survey Open-File Report 2005-1058
- Price AR, Jobbins G, Shepherd A, Ormond RF (1998) An integrated environmental assessment of the Red Sea coast of Saudi Arabia. *Environ Conserv* 25:65–76
- Rao KN, Subraelu P, Rao T, Malini B, Ratheesh R, Bhatta-charya S, Rajawat A (2008) Sea level rise and coastal vulnerability: an assessment of Andhra Pradesh coast, India through remote sensing and GIS. *J Coast Conserv* 12(4):195–207
- Roberts CM, McClean CJ, Veron JE, Hawkins JP, Allen GR, McAllister DE, Mittermeier CG, Schueler FW, Spalding M, Wells F, Ynne CV, Werner TB (2002) Marine biodiversity

- hotspots and conservation priorities for tropical reefs. *Science* 295(5558):1280–1284
- Saad A (2010) Wave and wind conditions in the Red Sea—a numerical study using a third generation wave model. M.Sc. Thesis in Physical Oceanography. Geophysical Institute, University of Bergen, Norway
- Saifullah SM (1994) Mangrove ecosystem of Saudi Arabian Red Sea coast—an overview. *J King Abdulaziz Univ Mar Sci* 7:263–270
- Sheppard CR (2003) Predicted recurrences of mass coral mortality in the Indian Ocean. *Nature* 425:294–297
- Simas T, Nunes J, Ferreira J (2001) Effects of global climate change on coastal salt marshes. *Ecol Model* 139:1–15
- Small C, Nicholls RJ (2003) A global analysis of human settlement in coastal zones. *J Coast Res* 19(3):584–599
- Thieler ER, Hammar-Klose ES (1999) National assessment of coastal vulnerability to sea level rise, U.S. Atlantic coast. U.S. Geological Survey, Open-File Report 99–593, 1 sheet
- Thieler ER, Hammar-Klose ES (2000) National assessment of coastal vulnerability to future sea-level rise: preliminary results for the U.S. Atlantic coast. U.S. Geological Survey, Open File Report 99–593, 1 sheet
- Tucker CJ (1979) Red and photographic infrared linear combinations for monitoring vegetation. *Rem Sens Environ* 8:127–150
- UNEP (United Nations Environment Programme) (1992) The world environment 1972–1992: two decades of challenge. Chapman & Hall, New York
- Vincent P (2008) Saudi Arabia: an environmental overview. Taylor & Francis Group, London
- Weiss JL, Gutzler DS, Coonrod A, Dahm CN (2004) Long term vegetation monitoring with NDVI in a diverse semi-arid setting, central New Mexico, USA. *J Arid Environ* 58:249–272
- Williams S (2013) Sea-level rise implications for coastal regions. *J Coast Res* 63:184–196